DOI: 10.3990/2.206

Rip Current Observations at Egmond aan Zee

G. Winter[1,2*], A.R. van Dongeren[2], M.A. de Schipper[1] and J.S.M. van Thiel de Vries[1,2]
[1]Faculty of Civil Engineering and Geosciences, Delft University of Technology, Delft, The Netherlands
[2]Deltares, Marine and Coastal Systems, P.O. Box 177, 2600 MH Delft, The Netherlands
*corresponding author: Gundula.Winter@deltares.nl

ABSTRACT

Rip currents are narrow, seaward directed flows in the surf zone that can pose a serious threat to swimmers. This issue has received attention particularly on swell dominated coasts (such as the US, Australia, France and UK) where numerous field experiments have been undertaken. However, the threat of rip currents is less recognised on wind-sea dominated coasts such as the North Sea, even though a consistent number of swimmers drift offshore (in rip currents) and require rescue by surf lifeguards each year (for example at Egmond aan Zee, The Netherlands). In August 2011, a five day field experiment SEAREX (Swimmer Safety at Egmond – A Rip current Experiment) was conducted. Lagrangian velocity measurements were taken with drifter instruments and human drifters that were tracked via GPS. Three flow patterns were observed in the experiment: (1) a locally governed circulation cell, (2) a pattern in which the drifter initially floats offshore and then is advected by a strong tidal alongshore-directed current and (3) a meandering longshore current between the shoreline and the bar. A variety of rip current velocities were measured with the strongest being approximately 0.6 m/s. The field data was hindcasted with the numerical model XBeach. Based on this model the sensitivity of rip currents towards wave height, water level and rip channel depth was investigated. Both field and model data show that offshore velocities in a rip increase with increasing wave height and decreasing water level, but that the rip channel depth imposes an upper limit on the rip current velocity.

INTRODUCTION

Rip currents are narrow, offshore directed flows that are generated by wave interaction or structural interaction mechanisms [*Dalrymple*, 1978]. The latter group consists of rip currents induced by the bottom topography, coastal boundaries (such as breakwaters and groins) as well as barred coastlines and are referred to bathymetrically controlled rip currents. This type of rip currents are found to be stronger than their non-morphologically controlled counterparts, the so-called transient rip currents [*Dalrymple et al.*, 2011]. This paper will focus on barred coastlines and the rip currents induced in this context.

The location of rip currents on a barred coast line is tied to a rip channel that interrupts the sand bar (Figure 1). Waves break over the bar, and exert a force on the water column through radiation stress gradients [*Longuet-Higgins and Stewart*, 1964]. This force causes a relatively high water level set-up in the trough between the beach and the bar. However, in the channel the waves break later (due to the deeper water) and induce less set up. The alongshore water level gradient initiates a longshore flow parallel to the beach that is referred to as feeder current. The feeder currents converge onshore of the rip channel into an offshore flow, the so-called rip neck. Outside the surf zone the rip current diffuses in the rip head. Together with the onshore mass transport over the sand bar the rip current forms a closed circulation cell.

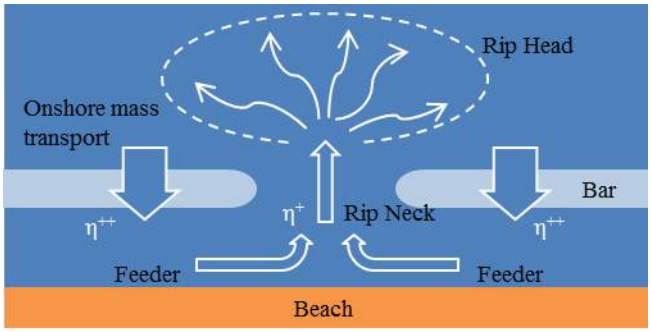

Figure 1. Rip current circulation cell. η++ indicates a relatively large water level set-up and η+ a relatively small set-up.

A number of field experiments have been undertaken to measure rip currents in the field with fixed instruments [*Aagaard et al.*, 1997; *Brander*, 1999; *Callaghan et al.*, 2004; *Dette et al.*, 1995; *MacMahan et al.*, 2005]. Current meters deployed in cross shore and/or longshore transects provide Eulerian flow measurements and give insight in the temporal variations of rip currents. However, the installation of these instruments in the surf zone is problematic and this experimental set-up provides limited spatial information about flow patterns of rip currents.

In more recent field studies GPS tracked drifters have been used to obtain a more comprehensive image of the flow patterns in a rip current and to overcome the limitations associated with fixed instrument transects [*Austin et al.*, 2010; *Johnson and Pattiaratchi*, 2004; *MacMahan et al.*, 2010]. People were also utilised as human drifters and were tracked either with two theodolites from the beach [*Brander and Short*, 2000] or with GPS trackers mounted to the people's heads [*MacMahan et al.*, 2010].

The results of GPS drifter tracking have shown that floating objects are mainly retained in the surf zone [*Reniers et al.*, 2009]. Observed flow patterns include eddies and meandering long shore currents [*MacMahan et al.*, 2010] and only infrequently is drifting material ejected offshore or washed on the beach.

This paper describes rip current characteristics on the Dutch coast and the results of the field experiment at Egmond aan Zee. The objectives of this research were to describe the rip current

flow patterns and to investigate the correlation of typical rip current velocities with hydrodynamic forcing.

A five day field experiment was conducted and the collected data was used to identify the governing parameters of rip current speed and to validate a hindcast model. The identified parameters were then subjected to a sensitivity analysis in the validated model.

This study contributes to the ultimate goal to predict rip currents based on forecasted hydrodynamic parameters given that an accurate bathymetry is available.

FIELD METHODS

In August 2011 (yeardays 234 – 238), a five day field experiment SEAREX (Swimmer safety in Egmond aan Zee – A Rip current Experiment) was conducted. The beach at the site is fronted by three bars of which the first and second are interrupted by several rip channels. Measurements were performed in two distinct rip channels in the second bar (Figure 2).

Lagrangian velocities in the surf zone were measured with drifter instruments that were similar to the design by *Schmidt et al.* [2003] (Figure 3). The drifters were tracked by GPS dataloggers and post-processed with data from a static base station to sub-meter accuracy following *MacMahan et al.* [2009]. In addition to the drifter instruments, human drifters were equipped with the same GPS units.

To distinguish regions of different flow intensities, the drifters were deployed in matrices consisting of two drifter rows either in alongshore or cross-shore direction. The drifters were deployed in cross-shore arrays when the updrift feeder was dominating.

A high resolution bathymetry survey was conducted using jetski and wheel-barrel mounted RTK-GPS instruments. Offshore wave data was recorded by an existing directional wave rider buoy at

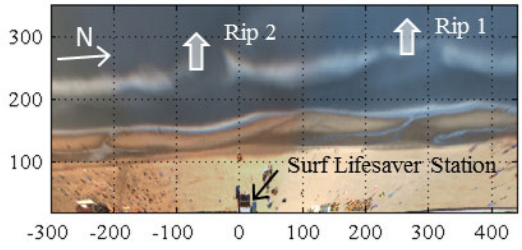

Figure 2. Argus plan view of the field site (derived from camera images taken from the lighthouse). The northern (Rip 1) and southern (Rip 2) rip channel are indicated.

Figure 3. Drifter instruments used during SEAREX.

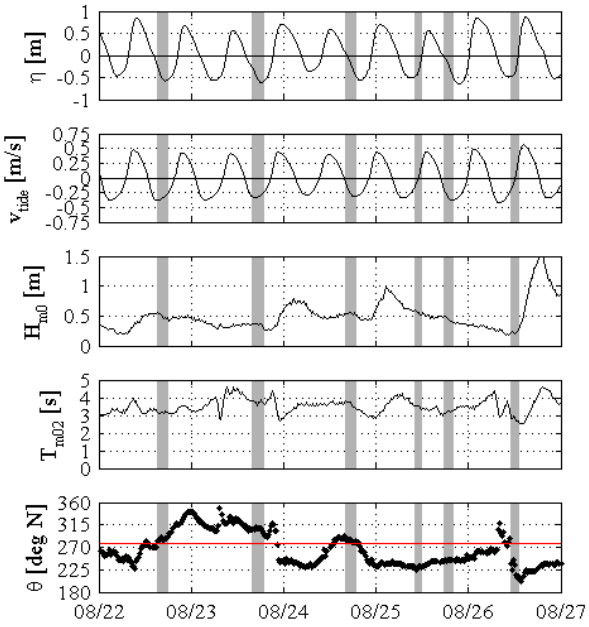

Figure 4. Hydrodynamic conditions during the field experiment from top to bottom: Water level (η) [m], tidal current (v_{tide}) [m/s], wave height (H_{m0}) [m], wave period (T_{m02}) [s] and wave angle (θ) [°N]. The red line in the bottom panel indicates the shore normal. The grey bars mark drifter experiments (with four to five deployments each).

Petten (maintained by Rijkswaterstaat) located 21 km North and 8.3 km offshore of the field site. Due to the relative uniformity of the coastal profile, wave data from this location is assumed representative for the offshore conditions at Egmond.

FIELD RESULTS

Hydrodynamic Conditions

The wave conditions were moderate throughout the experiment with the offshore wave height H_{m0} ranging from 0.35 to 0.7 m and the wave period T_{m02} ranging from 2.4 to 3.8 s. The field campaign coincided with neap tide with the smallest astronomical tidal range of 1.15 m on August 24. During the deployments the water level was around or below NAP +0 m. An overview of the tidal and wave conditions is provided in Figure 4.

Rip Current Velocities

An extensive dataset of rip current measurements in a Lagrangian framework was collected. In total, 28 drifter deployments were performed and 21 of these observations were classified as rip events. A rip event is defined as a flow pattern in which the drifters floated through the rip channel offshore.

The maximum drifter velocity of 0.60 m/s was measured on August 26 when also the highest offshore wave heights were recorded. The wave height H_{m0} was as large as 0.7 m and the offshore wave period T_{m02} was 3.6 s.

The offshore extent of the measured rip currents was in the order of 100 m offshore of the bar crest and stretched as far as 150 m. Large offshore extents were associated with strong offshore flows in which the drifters exited the surf zone. When the

drifters were retained in the surf zone the offshore extent was only 30 to 60 m offshore of the bar crest.

Observed Flow Pattern

In the experiment three flow patterns were observed: (1) a locally governed circulation cell (2) a pattern in which the drifter initially floats offshore and is then advected by the tidal longshore current and (3) a meandering longshore current. Pattern (1) and (2) describe rip events.

(1) The local circulation cell was always confined to the surf zone and was centred over the end of the downdrift bar (Figure 5). Only one circulation cell was observed downdrift of the channel while at no time during the experiment was a counter rotating eddy updrift of the rip channel observed.

(2) The drifters floated through the channel, exited the surf zone and were advected by a tidal longshore current offshore (Figure 6). The observed flow direction offshore of the bar was consistent with the tidal flow during those deployments. In case of weak tidal currents the drift direction was governed by the angle of wave incidence and/or the prevailing wind direction.

Flow pattern 2 was observed with rather high flow velocities in the rip channel (on average $u_{drifter}$ = 0.31 m/s compared to $u_{drifter}$ =

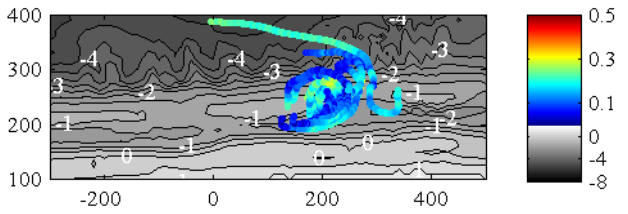

Figure 6. Local circulation cell measured during one deployment on August 22: The velocities are indicated by the colours and the bathymetry is plotted underneath in grey.

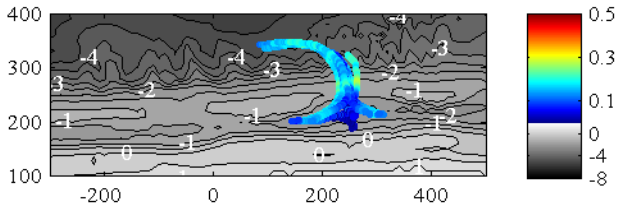

Figure 7. Offshore directed drifter paths during one deployment on August 23: The velocities are indicated by the colours and the bathymetry is plotted underneath in grey.

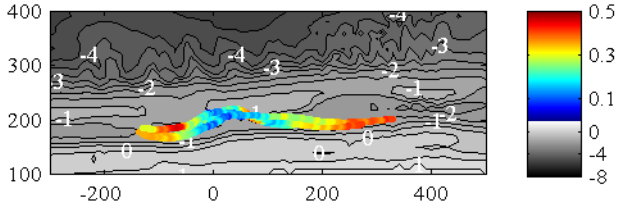

Figure 8. Meandering longshore current during one deployment on August 25: The velocities are indicated by the colours and the bathymetry is plotted underneath in grey.

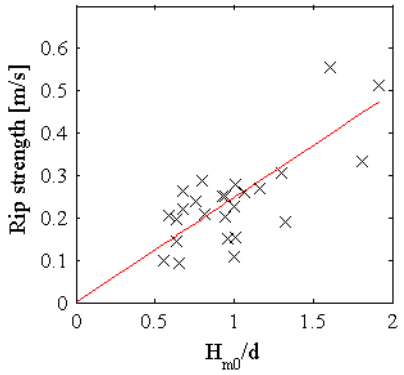

Figure 5. Rip strength versus H_{m0}/d. The solid red line represents the linear regression line.

0.18 m/s observed with flow pattern 1) and suggests that stronger currents possess enough inertia to enable the current (and the drifter) to exit the surf zone.

(3) The meandering longshore current is separated from (2) in the way that drifter paths are confined to the zone between the breaker bar and the beach (Figure 7).

This pattern was observed with water levels around or above NAP +0 m. The measurements were conducted in the presence of a northward directed tidal current. Both wind and waves came from southern directions and were likely to enhance the northward drifter movement.

FIELD DATA ANALYSIS

Correlation of rip currents with hydrodynamic forcing

Rip current flow is conditional upon wave dissipation. An indicator for the intensity of wave breaking is the ratio of the offshore wave height H_{m0} over the water depth on the bar d. The rip currents were evaluated in terms of the rip strength which represents the offshore velocity in a rip current. The rip strength is calculated by taking the maximum offshore velocities of each drifter that floated offshore in the rip channel and then averaging those values over one deployment.

A linear least squares regression was fit to the data with H_{m0}/d as independent variable and the rip strength as response variable (Figure 8). The R^2 value of the regression model is 0.68 and the p-value is 0.0048 and thus, a statistically significant correlation between the rip strength and wave height over water depth ratio is existent.

Correlation with Argus video images

The size of the data set does not allow drawing definite conclusions from a statistical analysis. In particular, it cannot be decided whether the high velocities measured on August 26 are outliers or indicate a trend (here they were not treated as outliers).

Therefore, a series of video images (Argus) that reveal areas of wave dissipation was used to examine the relation between H_{m0}/d and the rip strength. Figure 9 shows three images recorded on August 25 with low water level (large H_{m0}/d), intermediate water level and high water level (small H_{m0}/d).

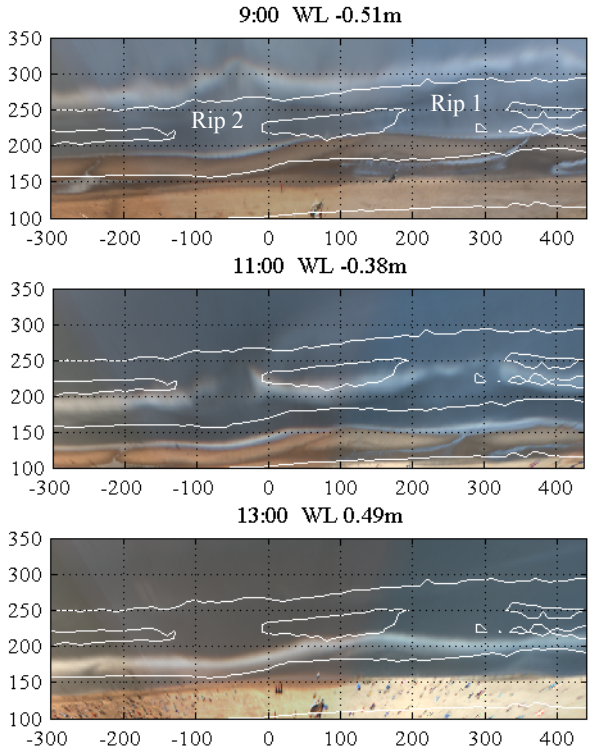

Figure 9. Series of Argus images on August 25. The water level increases from top to bottom and therewith the wave breaking shifts from offshore of the first surf zone bar to the swash bar. Wave breaking takes place slightly offshore of the white band that indicates the bores of the broken waves.

The statistical analysis indicated that the rip strength decreased with decreasing H_{m0} /*d*. The video images show that with higher water levels, the waves propagate over the surf zone bar and are not dissipated until they reach the swash bar (bottom panel). This interrupts the driving mechanism for rip currents on the first surf zone bar and explains the low rip activity with low values of H_{m0} /*d*. Similar observations were made in previous field studies where weak or no rip currents were measured at high tide [*Aagaard et al.*, 1997; *Austin et al.*, 2010; *Brander*, 1999].

However, the linear relation suggested in the statistical analysis may not hold for very low water levels (large H_{m0} /*d*) when the waves are also dissipated in the channel (top panel). As a consequence the longshore variation in wave dissipation and water level set up (which drive the rip current circulation) are weakened (Rip 2) or completely absent (Rip 1). An offshore current in Rip 2 is evident from the protuberance in the wave dissipation band. The opposing current causes the waves to refract towards the current and causes a non-uniform wave dissipation band.

The influence of the wave dissipation was further investigated in a sensitivity analysis using a numerical model (see below).

NUMERICAL MODEL

Hindcast

A hindcast model of the rip current system was built using XBeach [see *Roelvink et al.*, 2009 for a model description] in stationary mode (no wave group forcing). The drifter option was used to validate the model against flow patterns and rip current velocities observed in the field. From four out of five days one representative deployment was chosen to replicate in the hindcast model.

The hindcast model reproduced the field observations with respect to the rip strength well (Table 1). The large offshore velocities measured on August 25 are attributed to a cross-offshore wind that was not implemented in the model.

Likewise, the drifter trajectories were replicated well. Figure 10 shows the modelled drifter paths of a deployment on August 22 and August 23. The circulation and advection of the drifters to the South is reproduced well (compare with Figure 5 and Figure 6).

However, all hindcast models had in common that the offshore extent of the rip current was underestimated. This is attributed to the distinct vertical flow structure offshore of the rip channel with large offshore directed velocities near the surface and weak or slight onshore directed velocities near the bed [*Haas and Svendsen*, 2002]. This particular flow structure is not accounted for in a 2DH model and therefore, the offshore velocities in the upper water layer were underestimated. As a consequence, the drifters that floated in the upper water layer were advected less far offshore in the model than they were observed in the field.

Table 1. Rip strength calculated from the measured and modelled drifter data.

Deployment Day	Measured [m/s]	Model [m/s]
August 22	0.29	0.25
August 23	0.24	0.20
August 24	0.21	0.26
August 25	0.55	0.36

Sensitivity Analysis

The validated model was used to investigate the relation between H_{m0} /*d* and the rip strength in more detail. Several combinations of wave height, rip channel depth (with respect to the bar crest) and water level were tested (Figure 11). The model results also show an increase in rip strength with increasing H_{m0} /*d*. But the maximum possible rip strength is limited by the rip channel depth because it determines when wave breaking commences in the channel. It is thus not the wave dissipation on the bar, but the dissipation gradient from the bar to the channel that governs the strength of a rip current.

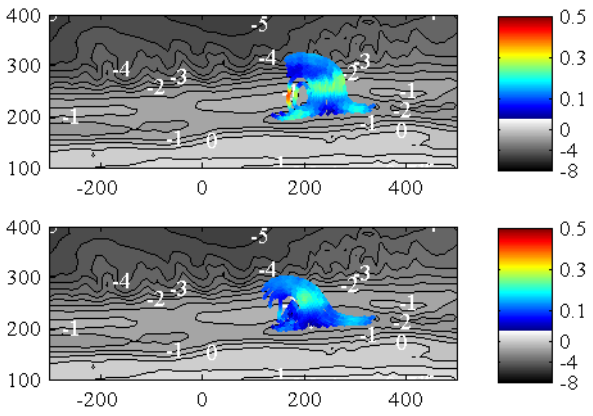

Figure 10. Modelled drifter paths of a deployment on August 22 (top) and August 23 (bottom).

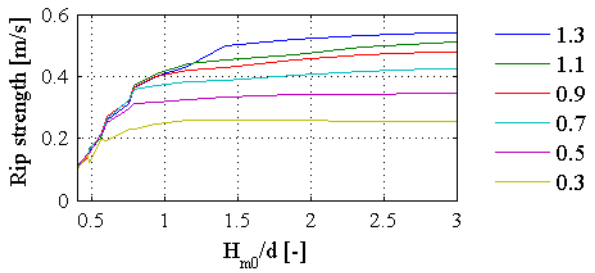

Figure 11. Rip strength vs. H_{m0}/d for various rip channel depths ranging from 0.3 m to 1.3 m.

CONCLUSIONS

A field experiment demonstrated the existence of rip currents at the wind-sea dominated coast of Egmond aan Zee with water levels below NAP +0 m. With water levels around or above NAP +0 m meandering longshore currents prevailed. Under moderate wave conditions (H_{m0} = 0.35 to 0.7 m) these rip currents reached a considerable strength of up to 0.6 m/s.

A statistically significant correlation between the measured rip current strength and the ratio of offshore wave height over water depth on the bar was identified. Video images indicate that this relation is not linear but stagnates for large values of H_{m0}/d when wave breaking commences in the rip channel.

A hindcast of the measurements was performed in the numerical model XBeach. The model showed good agreement with the field data in terms of the rip strength. The flow patterns were also replicated fairly well though the offshore extent of the rip current was consistently underestimated.

In the validated model the sensitivity of the rip strength to wave height, water level and channel depth was analysed and confirmed the conclusions drawn from the field data that rip strength increases with increasing H_{m0}/d until wave breaking commences in the rip channel which retards the rip current flow.

ACKNOWLEDGEMENT

We thank the many volunteers who assisted in collecting the field data: Andrew Pomeroy, Antoon Hendriks, Arnold van Rooijen, Brice Blossier, Claire Bouchigny, Cilia Swinkels, Dano Roelvink, Dirk Knipping, Erwin Bergsma, Giorgio Santinelli, Greta van Velzen, Hesseltje Roelvink, Ivan Garcia, Jamie Lescinski, Jeroen Stark, Lisa de Graaf, Leo Sembiring, Maarten van Ormondt, Roland Vlijm, Timon Pekkeriet and in particular Willem Verbeek whose experience with rip currents at Egmond aan Zee was valued highly.

We appreciate the help and equipment provided by Shore Monitoring and the bathymetry survey that was conducted by them. On site Shore Monitoring was represented by Roeland de Zeeuw and Sierd de Vries.

Rijkswaterstaat is gratefully acknowledged for the use of the wave buoy data taken at Petten that was provided to us by Andre Jansen.

The research was funded by Flood Control 2015 (Realtime Safety on Sedimentary Coasts program) and Building with Nature (Swimmer Safety project), Deltares Strategic Funding in the framework of the System Tools for Prevention and Preparation program (project 1202362).

M.A. de Schipper was funded by Building with Nature under project code NTW 3.2.

REFERENCES

Aagaard, T., B. Greenwood, and J. Nielsen (1997), Mean currents and sediment transport in a rip channel, Marine Geology, 140(1-2), 25-45.

Austin, M., T. M. Scott, J. W. Brown, J. A. Brown, J. H. MacMahan, G. Masselink, and P. Russell (2010), Temporal observations of rip current circulation on a macro-tidal beach, Continental Shelf Research, 30(1149-1165).

Brander, R. W. (1999), Field observations on the morphodynamic evolution of a low-energy rip current system, Marine Geology, 157(3-4), 199-217.

Brander, R. W., and A. D. Short (2000), Morphodynamics of a large-scale rip current system at Muriwai Beach, New Zealand, Marine Geology, 165(Compendex), 27-39.

Callaghan, D. P., T. E. Baldock, and P. Nielsen (2004), Pulsing and Circulation in Rip Current System, in International Conference Coastal Engineering, edited by J. M. Smith, pp. 1493-1505, American Society of Civil Engineers, Lisbon.

Dalrymple, R. A. (1978), Rip currents and their causes, in International Conference on Coastal Engineering, edited, pp. 1414-1427, American Society of Civil Engineers, Hamburg.

Dalrymple, R. A., J. H. MacMahan, A. J. H. M. Reniers, and V. Nelko (2011), Rip Currents, Annual Review of Fluid Mechanics, 43(1), 551-581.

Dette, H. H., K. Peters, and F. Spignat (1995), About rip currents at a meso-tidal coast, in Coastal Dynamics '95, edited, pp. 477-488, American Society of Civil Engineers, Gdansk, Poland.

Haas, K. A., and I. A. Svendsen (2002), Laboratory measurements of the vertical structure of rip currents, J. Geophys. Res., 107(C5), 3047.

Johnson, D., and C. Pattiaratchi (2004), Transient rip currents and nearshore circulation on a swell-dominated beach, J. Geophys. Res., 109(C2), C02026.

Longuet-Higgins, M. S., and R. W. Stewart (1964), Radiation stresses in water waves; a physical discussion, with applications, Deep Sea Research and Oceanographic Abstracts, 11(4), 529-562.

MacMahan, J. H., J. Brown, and E. Thornton (2009), Low-Cost Handheld Global Positioning System for Measuring Surf-Zone Currents, Journal of Coastal Research, 744-754.

MacMahan, J. H., E. B. Thornton, T. P. Stanton, and A. J. H. M. Reniers (2005), RIPEX: Observations of a rip current system, Marine Geology, 218(Compendex), 113-134.

MacMahan, J. H., et al. (2010), Mean Lagrangian flow behavior on an open coast rip-channeled beach: A new perspective, Marine Geology, 268(1-4), 1-15.

Reniers, A. J. H. M., J. H. MacMahan, E. B. Thornton, T. P. Stanton, M. Henriquez, J. W. Brown, J. A. Brown, and E. Gallagher (2009), Surf zone surface retention on a rip-channeled beach, J. Geophys. Res., 114(C10), C10010.

Roelvink, D., A. Reniers, A. van Dongeren, J. van Thiel de Vries, R. McCall, and J. Lescinski (2009), Modelling storm impacts on beaches, dunes and barrier islands, Coastal Engineering, 56(11-12), 1133-1152.

Schmidt, W. E., B. T. Woodward, K. S. Millikan, R. T. Guza, B. Raubenheimer, and S. Elgar (2003), A GPS-tracked surf zone drifter, Journal of Atmospheric and Oceanic Technology, 20(Compendex), 1069-1075.